Modal Analysis of a Sword

Garrett Dymond
Kettering University
Flint, USA
dymo0919@kettering.edu

Cale Gray
Kettering University
Flint, USA
gray8711@kettering.edu

Bailey Romo
Kettering University
Flint, USA
romo0096@kettering.edu

Mitchell Skiera
Kettering University
Flint, USA
skie1894@kettering.edu

Abstract

The intent of the testing performed was to identify and characterize the dynamic characteristics of a Viking-style sword in comparison to the theoretical dynamic characteristics of a comparably sized uniform rectangular bar of the same material. The position taken was that the free-free boundary condition model of a simple bar would serve as a comparable model to the behavior of said sword, with slightly reduced modal frequencies and distinct but similar mode shapes. The theoretical model of the free-free bar was first derived, and theoretical values for the modal frequencies were calculated. A computational model of the sword was developed and simulated using COMSOL Multiphysics, and modal frequencies were collected. Then, real experimental impact testing was performed on a test sword using a force hammer and accelerometers. Responses were recorded and then processed in Siemens TestLab. Upon the completion of these three mediums of exploration, the group found that the modal frequencies of the sword were in general lower than those of the bar, and the mode shapes were unique and dissimilar to those of the rectangular bar.

Introduction

Many modern-day objects are acoustically tested to better understand their use and inform design choices. Modal testing is the most common of the testing performed in these acoustic assessments, especially when it comes to objects that physically interact with other objects or the world they inhabit. Modal testing is the process of exciting objects, most done by way of physical impacts, in order to record and analyze the responses of the object to said excitements. When this is done the object will want to oscillate much more strongly at what is known as its modal or "natural" frequencies. At these frequencies, the object experiences its most significant distortion and tends to bend into some very characterizable shapes, modal shapes.

When it comes to objects that are more susceptible to resonating at their natural frequencies, look no further than the sword. A once-common armament of humankind dating back thousands of years, the sword is a tool that finds itself making impact often, and as such poses a rather interesting object to perform modal testing on. Over the years few studies have been undertaken when it comes to swords, as their status and prominence has fallen by the wayside in modern times, to say the least. One study however featured three different types of sword and attempted to characterize the first two vibrational modes for each of them. This study decided to model their objects with the free/free boundary conditions, and their goal by characterizing the modes was to determine whether or not there is a "sweet spot" where the sword can be struck to minimize the vibrations experienced by the user. The group found from the response that the sword is designed in a fashion such that the simple act of clasping the sword with the average size human hand provides adequate coverage for the multiple modes that appear in the hilt. On top of this, they found that the optimal location to strike at (the "sweet spot") was closer to the hilt for one blade and closer to the tip for the other in both mode cases (Marut, Michael, 2014). Studies on similar objects such as a cricket bat have also been conducted, and given that their use use of free/free boundary conditions allowed for them to model various modes for this similar object, we are confident that this is the proper set of conditions to perform the experimental analysis with (John and Li, n.d.). This will likely create differences when it comes to something like a computational model however, as more considerations such as the effect of the weight and geometry of the hilt become more relevant there and could require exploration of alternative boundary condition options.

This sweet-spot analysis is informative on the use-case of the sword, informing the user ideal strike locations and grip locations to minimize energy transfer between the sword and the user. This reduces the pain of heavy combat. In our study, we seek something slightly more fundamental to the sword object and less practical in nature. We will examine the impact of the geometry and mass distribution of the sword on its dynamic characteristics in comparison with a comparable rectangular bar. By first theoretically modeling a rectangular bar, identical to the sword's length, width, blade thickness, and material, a baseline free/free behavior will be established. Next, a computational model of the sword itself will be generated, making every attempt to replicate the sword as closely as possible. Finally, experimental modal analysis will be performed on a real sword (Figure 1), to observe the behaviors of the sword as they are. Once the data is collected, quantitative and qualitative analysis will imply the impact of the sword's geometry and mass distribution on its overall behavior in comparison with a rectangular bar. We predict that the impact of the geometry and mass distribution of a sword in comparison to a rectangular bar of similar geometry and composition will be generally reduced modal frequencies and distinct but similar mode shapes.

Figure 1: A Viking Sword to be used for experimental modal analysis.

Theoretical Model

When using a sword, it is free at both ends and thus a free-free boundary condition type should be used when doing modal analysis. When doing a theoretical model for the transverse mode shapes of a sword, the assumption is that the sword is the shape of a rectangular beam equal to the length of the sword. This will lead to some error, which is primarily due to the hilt being much larger than the blade of the sword. Nonetheless, modal analysis on rectangular bar with a width equal to that of the blade, will provide insight into the effects that the mass distribution and geometry have on a sword's mode shapes. For a free-free boundary condition rectangular bar, we start with the complete solution for the transverse mode shapes:

$$y = cos(\omega t)\left[Acosh\left(\frac{\omega x}{v}\right) + Bsinh\left(\frac{\omega x}{v}\right) + Ccos\left(\frac{\omega x}{v}\right) + Dsin\left(\frac{\omega x}{v}\right)\right]$$

At x = 0, the second and third derivative of y with respect to x are equal to zero. This implies that A = C, and B = D. This allows us to get the equation

$$y = cos(\omega t)\left[A\left(cosh\left(\frac{\omega x}{v}\right) + cos\left(\frac{\omega x}{v}\right)\right) + B\left(sinh\left(\frac{\omega x}{v}\right) + sin\left(\frac{\omega x}{v}\right)\right)\right]$$

Looking at the boundary condition at L, the second and third derivative are also equal to zero, so we have the system of equations:

$$A\left(cosh\left(\frac{\omega x}{v}\right)-cos\left(\frac{\omega x}{v}\right)\right)+B\left(sinh\left(\frac{\omega x}{v}\right)-sin\left(\frac{\omega x}{v}\right)\right)=0$$

$$A\left(sinh\left(\frac{\omega x}{v}\right)+sin\left(\frac{\omega x}{v}\right)\right)+B\left(cosh\left(\frac{\omega x}{v}\right)-cos\left(\frac{\omega x}{v}\right)\right)=0$$

Since the matrix is singular, the determinant equal zero and thus

$$cosh^2\left(\frac{\omega x}{v}\right)-2cos\left(\frac{\omega x}{v}\right)cosh\left(\frac{\omega x}{v}\right)+cos^2\left(\frac{\omega x}{v}\right)=sinh^2\left(\frac{\omega x}{v}\right)+sin^2\left(\frac{\omega x}{v}\right)$$

$$2cos\left(\frac{\omega x}{v}\right)cosh\left(\frac{\omega x}{v}\right)-2=0$$

$$cos\left(\frac{\omega x}{v}\right)cosh\left(\frac{\omega x}{v}\right)=1$$

We find the above equation equals zero, when $\frac{\omega x}{v}=\frac{\pi}{2}(3.0079,4.9961,6.9971,8.9981,10.9991,\ldots)$

Since $v=\sqrt{\omega c_1 \kappa}$, we have $\frac{\omega x}{\sqrt{\omega c_1 \kappa}}=\frac{\pi}{2}(3.0079,4.9961,\ldots)$, so $\sqrt{\omega^2}=\frac{c_1 \kappa \pi^2}{4x^2}(3.0079^2,4.9961^2,\ldots)$

and thus at x = L, we have $\frac{\omega}{2\pi}=f=\frac{c_1 \kappa \pi}{8L^2}(3.0079^2,4.9961^2,\ldots)$, which are the modal frequencies for the rectangular beam. At these frequencies, there will be maximal transverse displacement in the beam.

The constant $c_1=\sqrt{\frac{E}{\rho}}$, where $E = 250\ GPa$ is the Young's modulus measured in Pascals and $\rho = 7850\frac{kg}{m^3}$ is the material density. $\kappa=\frac{h}{\sqrt{12}}$ for a rectangular beam, and h is 0.5cm for the sword in question.

To get the final equation for the transverse waves at each of these modes, solve for B in the first equation from the system of equations, and plug it back into itself. Thus, we get

$$y=cos(\omega t)A\left[\left(cosh\left(\frac{\omega x}{v}\right)+cos\left(\frac{\omega x}{v}\right)\right)-\frac{cosh\left(\frac{\omega L}{v}\right)-cos\left(\frac{\omega L}{v}\right)}{sinh\left(\frac{\omega L}{v}\right)-sin\left(\frac{\omega L}{v}\right)}\left(sinh\left(\frac{\omega x}{v}\right)+sin\left(\frac{\omega x}{v}\right)\right)\right]$$

which is the equation for the transverse modes in a rectangular beam.

Computational Model

To computationally model the sword, one must first design it. From the Experimental Methods section, we see that the Viking sword is 74.5cm long, with a blade of length 57.2cm. The blade is 5.1cm wide at its widest point, and 3.9cm at its narrowest point. For simplicity sake, the blade is modeled with a uniform thickness of 0.5cm. Figure 2 shows the dimensions of the model that is used in the experiment.

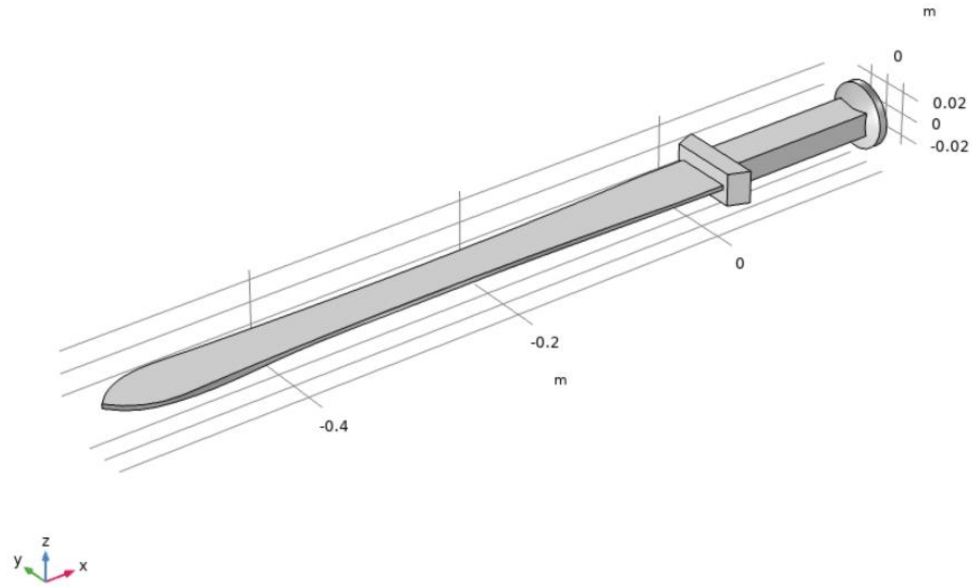

Figure 2: Model of a Viking sword with total length 74.5cm, blade length 57.2cm, blade width ranging from 3.9cm to 5.1cm, and blade thickness 0.5cm.

In the experimental section, the sword is made from solid steel. In the COMSOL model, the structural steel property is assigned to the sword. Structural steel has a Young's modulus of 200 GPa, and a material density of 7850 $\frac{kg}{m^3}$. No physics were added to the simulation because the sword is modeled by free-free boundary conditions. The sword was then meshed with a finer mesh. There were at least 2 mesh elements along the finest edge of the blade. The maximal modal frequency was 2610.9Hz, which leads to a wavelength of 13.2cm. The maximum element size was 4.1cm, so comparing it to the smallest wavelength, we are losing no information. COMSOL Multiphysics estimates the maximum error involved in its calculations for the phenomenon that is being simulated. The estimated error was $4 \cdot 10^{-15}$, which occurred in only one iteration. This suggests that there is very little error in our simulation at the nodes of the mesh. The simulation results are compared with theory and experiment, to confirm provide further credibility to the results of the simulation. Lastly, once the model was meshed, an eigenfrequency analysis of the first 25 modal frequencies was run on the model. The results can be summarized in Table 1.

Mode Number	Modal Frequency (Hz)	Mode Shape
1	30.54	Transverse
2	92.84	Transverse
3	206.99	Transverse
4	283.12	Torsional
5	314.41	Lateral
6	379.59	Transverse
7	610.10	Transverse
8	811.42	Torsional
9	896.97	Transverse
10	903.24	Transverse
11	1240.6	Transverse
12	1335.1	Torsional
13	1636.8	Transverse
14	1826	Lateral
15	1876.3	Torsional
16	2074.2	Transverse
17	2425.9	Torsional
18	2464.8	Transverse
19	2610.9	Longitudinal

Table 1: Modal Frequencies and Mode shapes for each of the modes in COMSOL Multiphysics.

An assumption for the modal analysis of the sword is that there are free-free boundary conditions. When compared with the theoretical model for a thin bar with the dimensions of the blade, the transverse modes seem to look different. Figure 3 shows the theoretical model for a thin bar in MATLAB, which models the blade of the sword using free-free boundary conditions, along with the COMSOL Multiphysics modal analysis for the whole sword. This discrepancy could be due to COMSOL modelling the sword blade, along with the hilt. The hilt is hypothesized to add some type of mass-loading condition to the theoretical model.

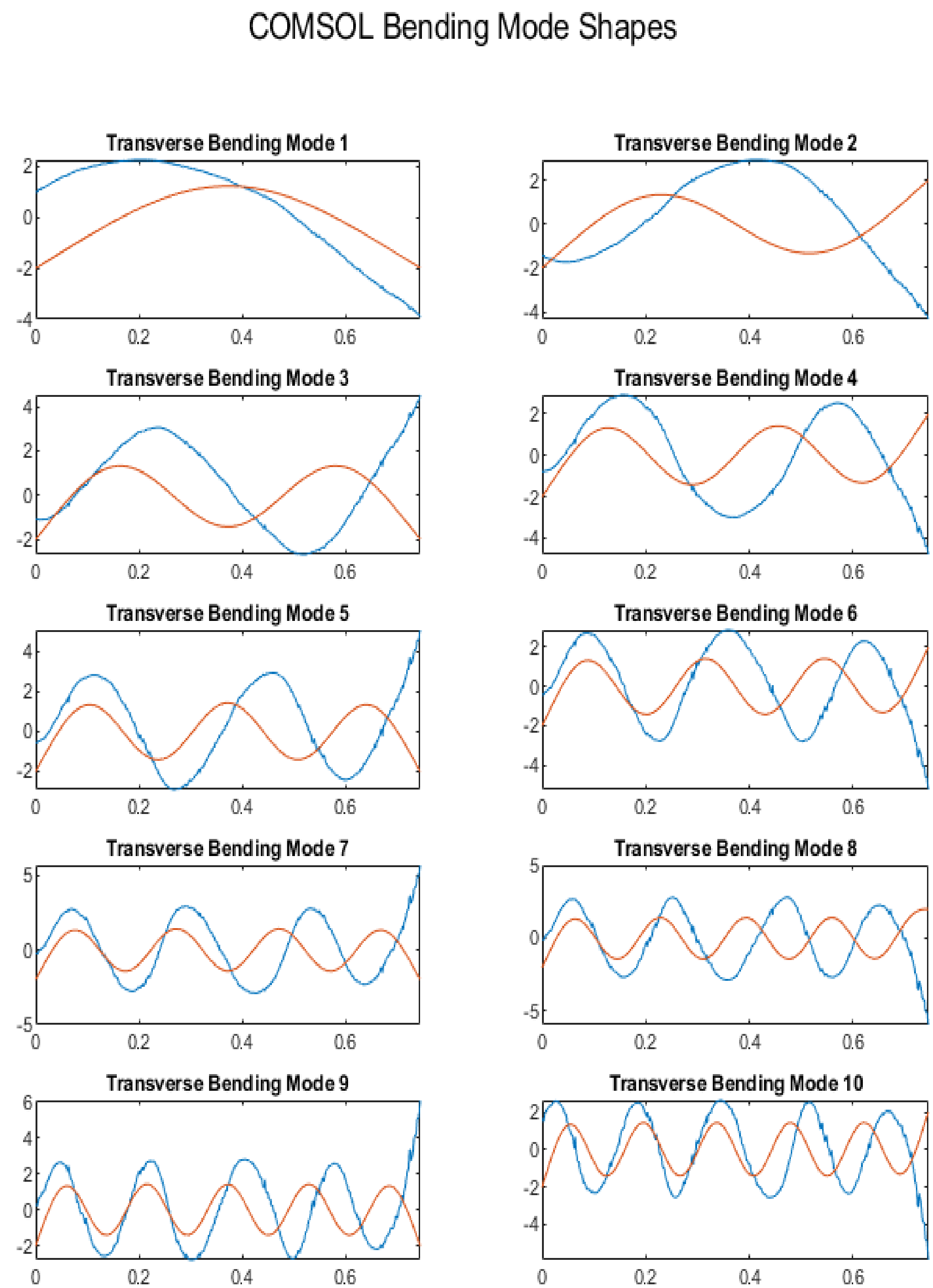

Figure 3: The theoretical (orange) transverse mode shapes in comparison to the computational (blue) transverse mode shapes.

Experimental Methods

Apparatus

The testing setup consists of a testing surface, which should be of adequate size and structure to ensure that there is no interference with results. As seen in Figure 4, a large metal table should suffice. The testing surface should also have uprights, in which four rubber bands can be used to stabilize the sword. The rubber bands are used to simulate the free-free boundary conditions. Next, a force hammer (PDC 086C02) with a hard, white plastic tip with a sensitivity of 2.25mV/N was attached to channel 1 of the data acquisition unit. Three “Teardrop” accelerometers (PCB 253C22) were placed on the test object at points 1, 3 and 64. The accelerometer is used to gather the measurements for the experiment. The accelerometers should have a sensitivity of 10mV/g, and should be attached to channels 2, 3, and 4 of the data acquisition unit. Lastly, the Siemens SCADAS data acquisition unit, along with Siemens LMS testlab are used to gather and interpret the measured data.

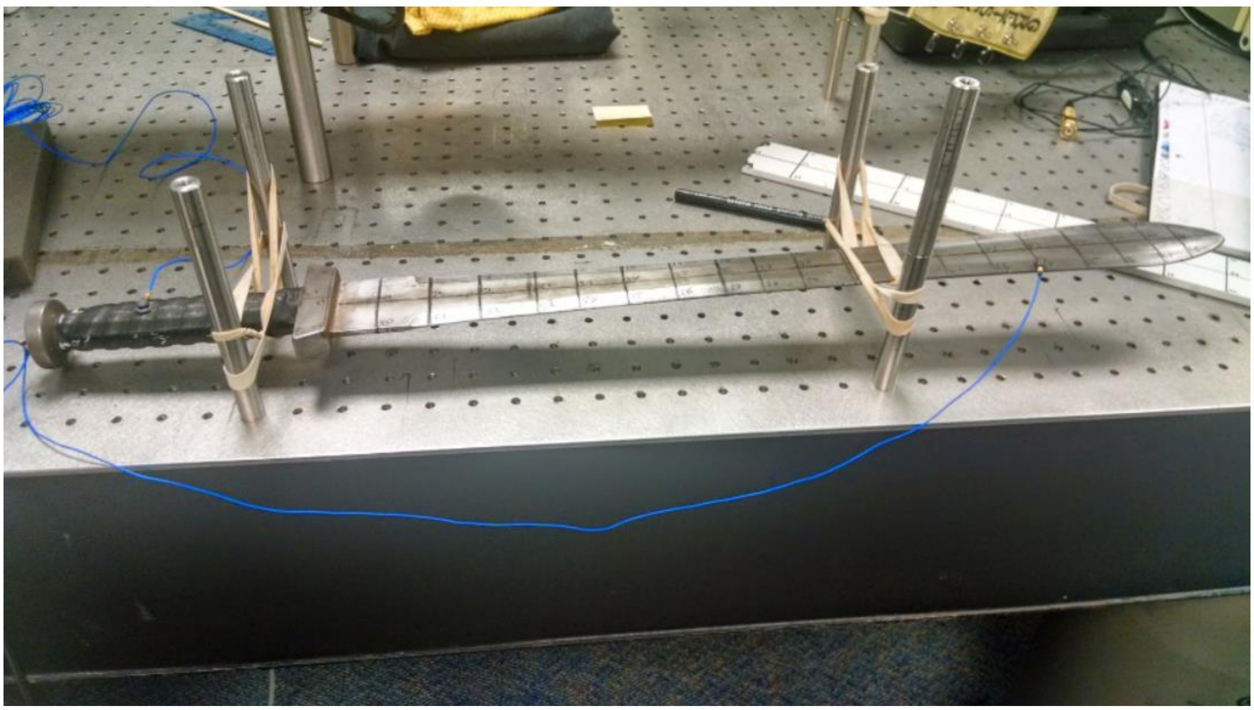

Figure 4: Experimental setup to test modal characteristics.

Procedure

The test surface was prepared by ensuring it was clear and that the uprights were spaced evenly and provided enough room for the test object to be mounted. The test object was prepared by marking the various locations along the length of the blade (about 57.2cm) that will be struck with the force hammer. These were spaced out such that there were 76 total points; 3 of which (1, 3, and 64) were used as the placement locations of the accelerometers and the other 73 of which served as actual test points. These were marked such that there were three main rows of points across the width of the blade; two along the lengths of each edge of the blade and one that ran along the length of the center of the sword. Next the

Accelerometers were calibrated and then placed on the aforementioned points 1, 3, and 64 of the object. Now the test object was fixed using the rubber bands attached between the uprights on the test surface to support the ends of the sword and keep them free in the air during testing. The test object was placed as level as possible between the uprights and resting on the rubber bands. The force hammer was calibrated and cleaned in preparation for its impact testing; the data acquisition unit was similarly checked on and prepped. With all of the equipment prepared, data was collected. The force hammer was used to excite the sword at each of the 73 points. Three sets of data were collected and averaged to produce results. Once data was collected, it was taken into Siemens Testlab for analysis and interpretation. The data was first selected in the “Modal Data Selection” tab and then taken into the “Time MDOF” tab in order to produce a Bode plot of the FRFs at each point as well as a Stabilization plot to determine relevant modal frequencies and their damping values. It will then be assessed and validated using the “Synthesis” and “Validation” tabs, such that conclusions and comparisons to the other aspects of the study can be drawn.

Experimental Results

With the experiment carried out and data collected, more tangible results can be produced, and subsequent interpretation/evaluation can then be conducted. As stated before, the data was first taken into Siemens TestLab and selected using the “Modal Data Selection” tab. Then the “Time MDOF” tab was opened with the appropriate data now selected, so that a Bode plot with each FRF could be produced. This plot can be seen below in Figure 4.

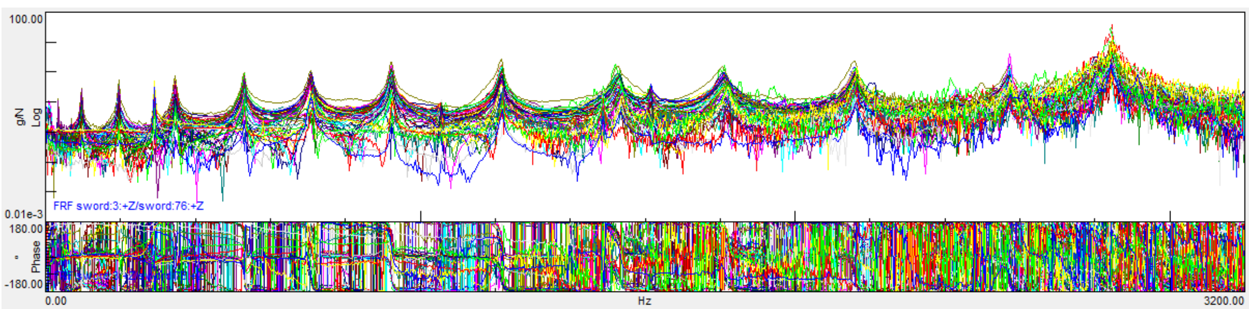

Figure 5: Bode Plot of FRFs from each of the 73 points on the object, produced in the “Time MDOF” tab in Siemens TestLab.

This plot is a lot to take in on its own, thanks to the amounts of data points it contains, however by selecting “stabilization” in the top ribbon of the tab we created a stabilization plot that better allowed us to identify and measure each of the relevant modes location in frequency as well as their damping values in percentage. This stabilization plot can be seen below in Figure 5.

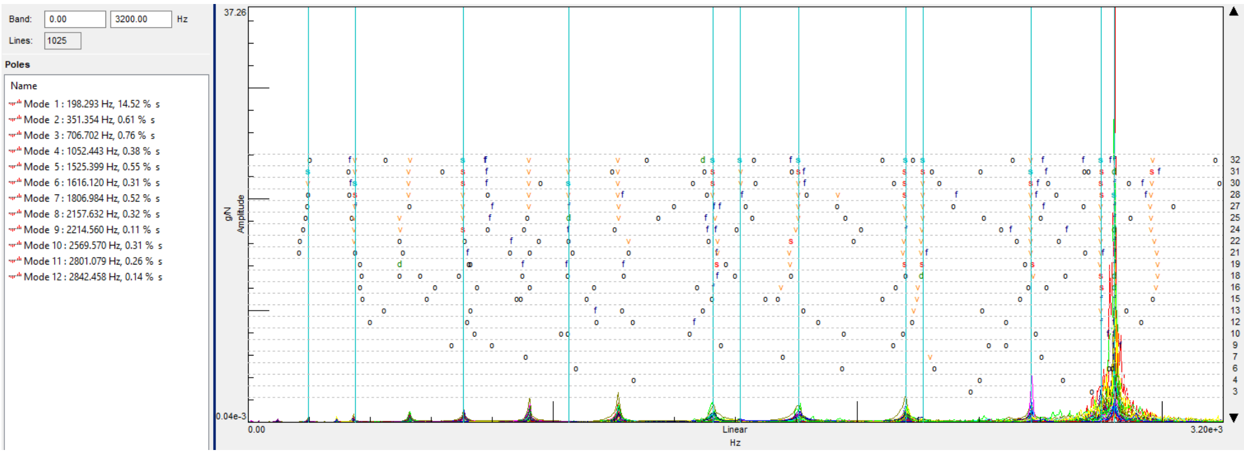

Figure 6: Stabilization plot produced in TestLab showing the locations of each of the 12 most relevant modes.

From the stabilization plot, we selected 12 modes based upon the letters given at each of the visible peaks on the plot (with tolerances of 4% and 6% for Vector and Damping, respectively). The peaks that had an ‘S’ above them were selected specifically, as the ‘s’ indicates that the Frequency, Damping, and Mode Shape results are stable within the set tolerances. The values for these 13 modal frequencies as well as their damping can be seen in Table 2. The three-dimensional shapes were also assessed, using the “shapes” ribbon option also found in the “Time MDOF” tab, and can be seen below in Figure 6.

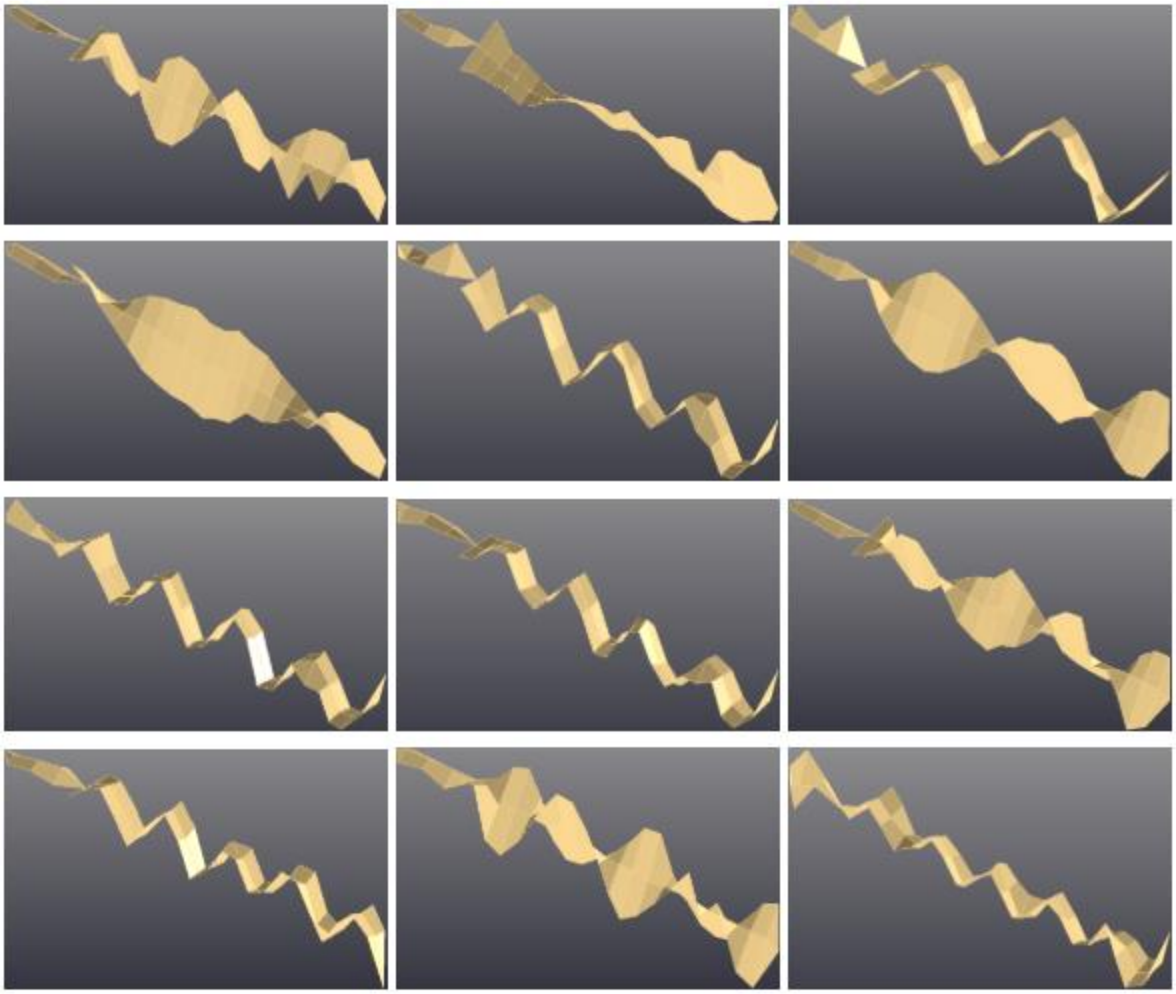

Figure 7: Modes shape results for all 12 of the relevant modes from the experiment. By type (from top-left to bottom-right): Transverse (3, 5, 7, 8, 10, 12); Torsional (1, 2, 4, 6, 9, 11).

Of the twelve total modes observed and plotted, six were found to be Transverse modes and the other six were found to be Torsional modes. In order to ascertain the validity of these results, validation was performed through the use of the “Modal Validation” tab, which allowed us to select all of our chosen modes as well as the FRF information from the recorded data, and compare the two to see how well they matched one another. The resulting “Stability” plot can be seen below in Figure 7. The Correlation value obtained from this plot was recorded to be 63.98% with an associated error of 36.76%.

Mode Number	Modal Frequency (Hz)	Damping Value (%)	Mode Shape
1	198.293	14.52	Torsional
2	351.354	0.61	Torsional
3	706.702	0.76	Transverse
4	1052.443	0.38	Torsional
5	1525.399	0.55	Transverse
6	1616.120	0.31	Torsional
7	1806.984	0.52	Transverse
8	2157.632	0.32	Transverse
9	2214.560	0.11	Torsional
10	2569.570	0.31	Transverse
11	2901.079	0.26	Torsional
12	2842.458	0.14	Transverse

Table 2: Condensed results information from the experimental data including Mode number, frequency, damping value, and type.

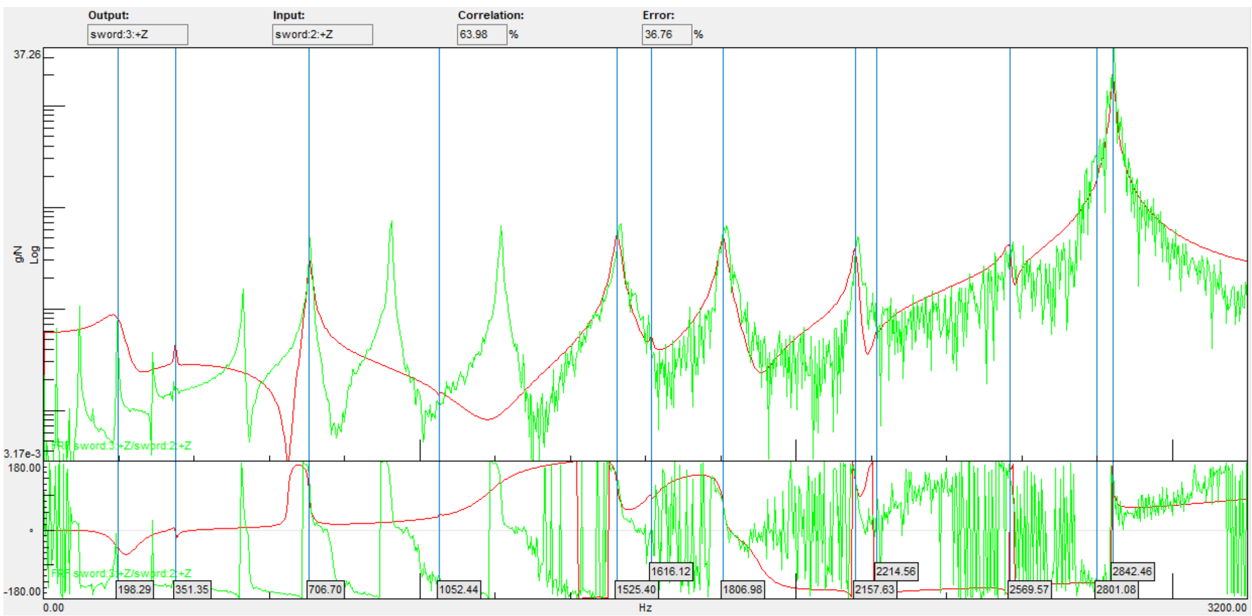

Figure 8: Stability Bode plot comparing the modes to the FRFs of the data points, produced in Siemens TestLab.

Discussion

In comparing the theoretical model, computational model, and experimental results, several key factors must be considered. First, the theoretical model is of a rectangular bar of the same length and width as the sword, with the thickness of the blade along the entire length of the bar. Obviously, this is a relatively poor approximation of what a sword is, and as such will output different values than one would expect from a real sword. The results are useful in terms of qualitative comparison, to understand the effects the geometry and mass distribution of a sword have on a free/free rectangular beam's dynamic characteristics. COMSOL Multiphysics attempted to simulate these characteristics more thoroughly, using finite elements of mass to numerically evaluate a solution. With finite element analysis, mesh choice, truncation error, and material property differences can introduce error. The experimental results have their own limitations: sensor calibration, accelerometer mass-loading, suspension system effects, window functions/aliasing, uncertainty propagating through all signal processing and postprocessing operations, and last but not least human error. With all of this in mind, comparison of the results can be done intentionally.

The three most important dynamic characteristics of any system are modal frequencies, mode shapes, and damping parameters. For the purposes of this study, only the modal frequencies and mode shapes were examined.

Transverse Mode Number	Theoretical Modal Frequency	COMSOL Modal Frequency	Experimental Modal Frequency
5	622.83	610.10	706.70
8	1668.00	1636.80	1525.39
9	1858.50	2074.20	1806.98
10	2270.40	2464.80	2157.63
11	2723.40	2738.90	2569.57
12	3271.60	3237.10	2842.45

Table 3. Comparison of transverse modal frequencies among the three different models examined

Table 3 shows the modal frequencies predicted by the theoretical and computational models in comparison with the experimentally measured modal frequencies. None are completely in agreement; but the theoretical derivation and COMSOL generally agree with each other well. Notably, the experimental modal frequencies are lower across the board than their modeled counterparts. Furthermore, the differences between modal frequencies in general are larger than typical differences between theory and data in scientific studies. This is largely due to the amount of opportunities for error in a modal analysis and illustrates the importance of theoretical and computational modeling in parallel with physical modal testing. Given what is known about each model, expected error also accounts for some of the difference between theory and data. Unfortunately, when trying to quantify this expected error, the error from other sources clouds the measurement. For this reason, it is possible to conclude in a very general way that the addition of the hilt, handle, and pommel to the theoretical model would result in lower modal frequencies. This follows the logical conclusion that the addition of more mass to a system, in the absence of other changes, would reduce the response to an input in terms of both amplitude and frequency as higher inertia would resist larger/faster changes in displacement.

Comparing the mode shapes of a free/free bar approximating a free/free sword and the simulation/experimental data of the same sword sheds light on the potential impacts of the sword's geometry and mass distribution. Examining Figure 3, there are significant behavioral differences between a rectangular bar and a sword. Primarily, there is an increasingly large difference (with respect to frequency) in the number of maxima and minima. This is due to the effects of the extra mass in the hilt of the sword. The hilt of the sword is located at $x = 0$ for the COMSOL model in Figure 3. It seems the first COMSOL mode shape is a slightly cut off version of the free/free mode shape, losing a little bit of the beginning. This pattern seems to continue throughout the spectrum of tested frequencies, with more and more being "cut off" as the frequency increases. This again follows the logical conclusion that the addition of mass to one side of the examined system would have the effect of making that end more lethargic in its response to input than the other.

In comparing the experimentally measured mode shapes with those calculated using theory and simulated by COMSOL, it becomes clear that the experimental data has error. There are several low-frequency modes that have multiple regions of significant opposite displacement, a phenomenon that should not generally occur. Furthermore, only some of the measured mode shapes match up with those predicted. It is reasonable to expect mode shapes to appear in the same order they do for the simulation (as frequency increases), so the fact that this does not occur indicates the data taken has enough error to report false behavior in the object.

Previous studies have examined these modal frequencies and mode shapes for the purposes of identifying and quantifying a “sweet spot” and its benefits (Marut, K. and Michael, T., 2014). Primarily, these studies found that the first modal frequency of a comparable sword is around 20 - 30 Hz (Marut, K. and Michael, T., 2014), which isn’t necessarily illuminating in terms of their goal. “Sweet spot” analysis isn’t as interested in the modal frequency as it is the mode shape and node location. In the case of this study, the first experimentally measured modal frequency was 198 Hz, a torsional mode. It is safe to say, given previous studies, theoretical and computational modeling, and intuition, that the experimental analysis missed a few modes in the lower end of the frequency spectrum. Otherwise, the first measured modal frequency would likely be some tens of Hz and its mode shape would shed some light on how this study compares with those researched in preparation for this experiment, as that is the most relevant data for comparison to a “sweet spot” analysis.

Conclusion

Upon comparing the theoretical calculations, with the computational and test data, it doesn’t appear that the sword behaves solely as a free-free body. A fixed end may be a more appropriate boundary for a sword, as this is how a cricket bat was modelled for computational testing performed by Sabu John, and Zhu Bang Li, in their journal. “Multi-directional Vibration Analysis of Cricket Bats”. Though projects like that of, Rod Selfridge, David Moffat, and Joshua D. Reiss, “Real-Time Physical Model for Synthesis of Sword Sounds”, are not concerned with the vibrations of the hilt of the sword, but rather just that of the blade. This may cause a free-free model to be correct, when just testing the blade, the difficulty would be being able to isolate the hilt during the impact testing.

Concerning the hypothesis stated earlier in the study, we were unable to properly correlate the theoretical and computational modeling with the experimental data. Therefore, we cannot draw any specific conclusions in terms of whether our hypothesis was true. We can, given the study of previous literature and our theoretical and computational model say in general terms that current research indicates that a sword has lower modal frequencies than a comparable thin metal bar due to the swords geometry and (primarily) mass distribution.

The end conclusion of this experiment is that a sword does not behave purely as a free-free body, when concerning model frequencies. A theoretical derivation of a mass loading end may lead to a closer approximation of the behavior. Further testing will need to be performed, to confirm that the blade itself behaves as free-free, when separated from the hilt, or if the whole sword behaves closer to a fixed or mass-loaded end. This additional data collection and experimentation would illuminate further the impact of the geometry and mass distribution on the modal parameters for a sword.

References

Kenneth Marut and Tyler Michael, (2014) "Unsheathing the Vibrational Dynamics of Swords,"

Sabu John & Zhu Bang Li. "Multi-directional Vibration Analysis of Cricket bats," Engineering, (Bundoora, Australia), Vic. 3083

Rod Selfridge, David Moffat, & Joshua D Reiss. (2017). "Real-Time Physical Model for Synthesis of Sword Sounds". Sound and Music, (Espoo, Finland), SMC2017-300--SMC2017-302

George L. Turner (2002) “The Modes and the Nodes of Vibration,” in *Dynamics of Hand-Held Impact Weapons*, Martial Arts, pp. 130-137.

R. S. Mohan, A. Sarkar, A. S. Sekhar (2014), “VIbration analysis of a steam turbine blade”, Engineering, (Madras, India), 1-10